tvst

https://doi.org/10.1167/tvst.7.3.11

Article

Comparison of Widefield and Circumpapillary Circle Scans for Detecting Glaucomatous Neuroretinal Thinning on Optical Coherence Tomography

Zhichao Wu[1–3], Denis S. D. Weng[1], Abinaya Thenappan[1], Rashmi Rajshekhar[1], Robert Ritch[4], and Donald C. Hood[1,5]

[1] Department of Psychology, Columbia University, New York, NY, USA
[2] Centre for Eye Research Australia, Royal Victorian Eye and Ear Hospital, East Melbourne, Australia
[3] Ophthalmology, Department of Surgery, The University of Melbourne, Melbourne, Australia
[4] Einhorn Clinical Research Center, New York Eye and Ear Infirmary of Mount Sinai, New York, NY, USA
[5] Department of Ophthalmology, Columbia University, New York, NY, USA

Correspondence: Zhichao Wu, Centre for Eye Research Australia, Level 7, 32 Gisborne St, East Melbourne, VIC 3002, Australia. email: wu.z@unimelb.edu.au

Received: 21 December 2017
Accepted: 23 April 2018
Published: 4 June 2018

Keywords: glaucoma; optical coherence tomography; progression; widefield

Citation: Wu Z, Weng DSD, Thenappan A, Rajshekhar R, Ritch R, Hood DC. Comparison of widefield and circumpapillary circle scans for detecting glaucomatous neuroretinal thinning on optical coherence tomography. Trans Vis Sci Tech. 2018;7(3):11, https://doi.org/10.1167/tvst.7.3.11

Purpose: Our purpose was to compare the effectiveness of detecting progressive retinal nerve fiber layer (RNFL) thickness changes using widefield scans compared to circumpapillary circle scans derived from optic disc volume scans when using a manual region-of-interest (ROI) approach.

Methods: In a prospective observational study, a total of 125 eyes diagnosed clinically with glaucoma or suspected glaucoma that had both widefield (12 × 9 mm) and optic disc (6 × 6 mm) scans obtained at least one year apart were included. Changes in the RNFL thickness between the two visits were evaluated within region(s) of observed or suspected glaucomatous damage, which were manually outlined after reviewing key features from each scan on the second visit (described as a manual ROI approach). Within ROI(s), changes in the widefield and circumpapillary RNFL thickness ($wfRNFL_{ROI}$ and $cpRNFL_{ROI}$), as well as in the global circumpapillary RNFL thickness ($cpRNFL_G$), were determined. The performance of these three methods for detecting progressive changes was compared using longitudinal signal-to-noise ratios (SNRs), whereby the rate of change determined by each method was normalized by individualized estimates of measurement variability and age-related change.

Results: On average, the longitudinal SNRs for the $wfRNFL_{ROI}$, $cpRNFL_{ROI}$, and $cpRNFL_G$ methods were −0.57, −0.38, and −0.23 y^{-1}, respectively, being significantly more negative for the $wfRNFL_{ROI}$ than the latter two methods ($P \leq 0.009$).

Conclusions: Progressive RNFL thickness changes were more effectively detected on widefield optical coherence tomography (OCT) scans using a manual ROI approach compared to conventional derived circumpapillary circle scans.

Translational Relevance: Widefield OCT scans show promise for improving the detection of glaucomatous progression.

Introduction

Optical coherence tomography (OCT) imaging has emerged in recent years as a powerful tool for characterizing and monitoring neuroretinal loss in eyes with glaucoma.[1] An accumulating body of evidence has shown its value for detecting glaucoma progression in both clinical practice[2–4] and its applications for clinical trials.[5,6]

Thus far, circumpapillary retinal nerve fiber layer (cpRNFL) thickness measurements have been the primary means for monitoring glaucomatous progression on OCT imaging, obtained either by acquiring circle scans or deriving them from optic disc volume scans. Some studies have also used retinal nerve fiber layer (RNFL) thickness measurements

from the entire volume scan of the optic disc (covering a 6×6-mm region) for detecting progression.[9–12] More recent studies have explored whether a "widefield" (12×9 mm) scanning protocol, which covers three times the area of these conventional optic disc volume scans, could be useful in the detection of glaucomatous damage at cross-section.[13–16] However, the value added of such widefield scans for detecting progressive RNFL thinning compared to the conventional circle scans remains unexplored. Since the RNFL contains axons from the retinal ganglion cells (RGCs) damaged in glaucoma, OCT widefield scans might allow RNFL thinning to be characterized over a substantially larger proportion of the entire RGC axonal tract, rather than sampling it at a single location within circumpapillary circle scans.

Therefore, this study compared cpRNFL thickness measurements from optic disc volume scans to RNFL thickness measurements from widefield scans in their ability to detect progressive changes after accounting for age-related changes and measurement variability. We enlisted a region-of-interest (ROI) approach for examining such progressive changes, as we have previously shown the advantages of such a method compared to global thickness measures.[17,18]

Methods

This was a prospective longitudinal observational study designed to improve the understanding of the role of OCT imaging in glaucoma, and it was approved by the Institutional Review Boards of Columbia University and the New York Eye and Ear Infirmary of Mount Sinai. It adhered to the tenets of the Declaration of Helsinki and the Health Insurance Portability and Accountability Act, and all participants included in this study provided written informed consent.

Study Overview and Outcome Measure

We compared three methods for detecting progressive RNFL changes in glaucoma eyes with two different OCT scanning protocols, as illustrated in Figure 1. The first method, which represents the most common approach clinically, evaluated the global cpRNFL thickness from a 6 × 6-mm optic disc volume scan ($cpRNFL_G$), whereas the second method evaluated the average cpRNFL thickness in a manually outlined ROI from the same scan ($cpRNFL_{ROI}$). The third method evaluated the average RNFL thickness within a manually outlined ROI from a 12 × 9-mm widefield volume scan ($wfRNFL_{ROI}$). These methods were used to evaluate RNFL thickness changes in a cohort of glaucoma eyes with these two OCT scans at least one year apart (longitudinal group). Measured changes for each method were normalized to enable equivalent comparisons between them after accounting for individualized estimates of measurement variability (from a variability group) and normal age-related changes (from a normative group). These normalized values were referred to as longitudinal signal-to-noise ratios (SNRs), and were used as the primary outcome measure in this study.

Participants

This study included two categories of participants: healthy participants and those with a clinical diagnosis of suspected or established glaucoma based on a comprehensive examination (including a clinical examination of the optic nerve appearance) by the referring glaucoma specialist (RR). Eyes with retinal pathology that could affect the inner retina (e.g., epiretinal membranes) were excluded. All these eyes were also required to have a reliable visual field test obtained using the Swedish Interactive Threshold Algorithm (SITA) Standard 24-2 testing strategy on a visual field analyzer (Humphrey Field Analyzer II-I; Carl Zeiss Meditec, Inc., Dublin, CA). A visual field test was defined as being unreliable if it had >15% false-positive errors, >33% fixation losses, or >33% false-negative errors (except when the mean deviation [MD] was less than −12 dB for the latter). Otherwise, the results of the visual field test were not used as an eligibility criterion for the participants with established or suspected glaucoma in this study, and we did not seek to distinguish between the two since the primary outcome analyzed in this study is the comparison of the three methods for detecting progressive RNFL thickness change within the same eye.

Healthy participants were also included and were originally included in reference database studies by the OCT device manufacturer (data were provided by Topcon, Inc., Tokyo, Japan). One eye was randomly selected from each participant, and they were all required to have a best-corrected visual acuity of 20/40 or better; have an intraocular pressure of ≤21 mm Hg; and be free of any ocular pathology, narrow angles, or a significant medical history that could influence test results. These eyes were also required to be free from visual field defects consistent with glaucoma on a visual field test when using the SITA Standard 24-2 strategy. These eyes were used to

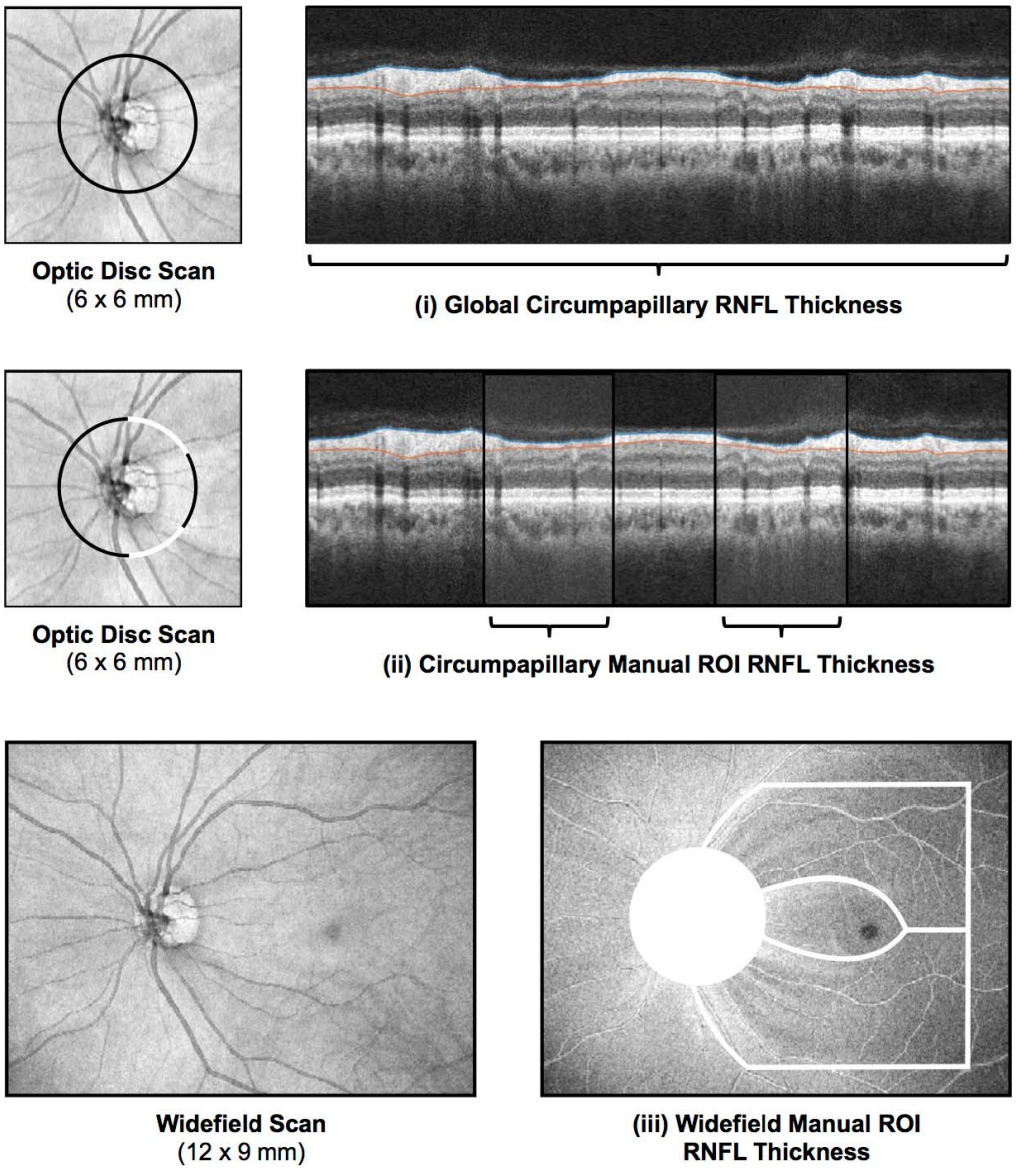

Figure 1. Illustration of the three methods of detecting the progression of RNFL thickness changes, including (i) cpRNFL thickness from an optic disc volume scan, (ii) average cpRNFL thickness in a manually outlined ROI (*black rectangles*) from the optic disc volume scan, and (iii) average RNFL thickness from a manually outlined ROI on a widefield scan (*white outlines*).

provide values for age-related changes in RNFL thickness for each of the methods evaluated in this study and were referred to as the normative group.

OCT Imaging

A widefield volume scan consisting of 512 × 256 A-scans covering a 12 × 9-mm region, including both the optic disc and macula, were obtained for all glaucoma eyes using a swept-source OCT device (Atlantis DRI OCT-1; Topcon, Inc.). A volume scan centered on the optic disc consisting of 512 × 128 A-scans covering a 6 × 6-mm region were also obtained for all eyes using a spectral-domain OCT device (3D OCT-2000; Topcon, Inc.). Any scan with significant blink or eye movement artifacts were excluded, and the automatic retinal layer segmentation from the device was used (without manual corrections, to ensure the results were as representative of a clinical practice scenario as possible). The glaucoma eyes were required to either have two of each type of scans obtained at least 1 year apart to determine longitudinal change (signal) or have two of each type of scans within the same visit to obtain test-retest variability estimates (noise). The eyes that satisfied these criteria formed the longitudi-

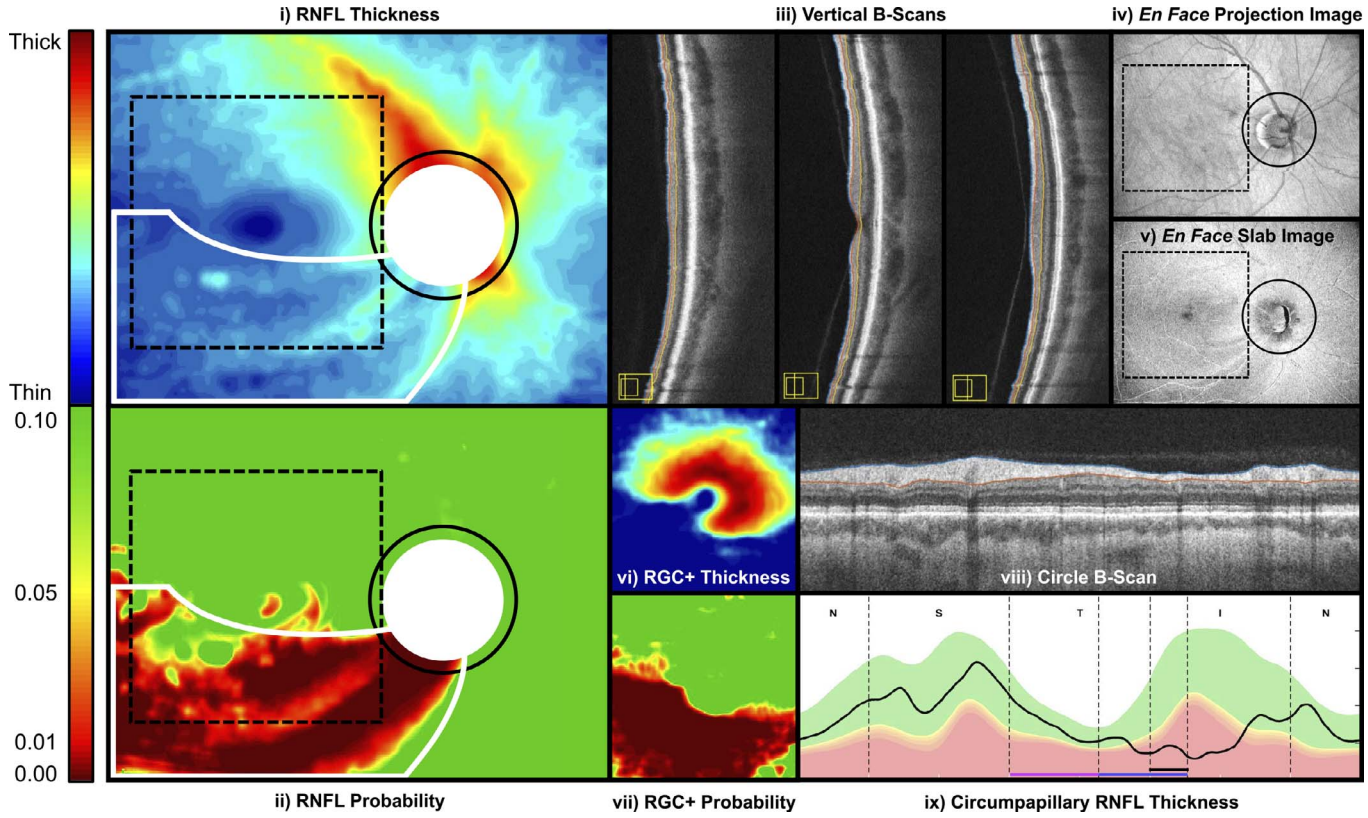

Figure 2. Information from the widefield scan evaluated when manually identifying a ROI, including (i) RNFL thickness map; (ii) RNFL thickness deviation probability map; (iii) three vertical line scans (taken through the fovea and ±1.5 mm on either side); (iv) en face projection image; (v) en face slab image of the inner retina; (vi) RGC plus inner plexiform layer (RGC+) thickness plot; (vii) RGC+ thickness probability plot; (viii) circumpapillary circle B-scan; (ix) circumpapillary RNFL thickness profile. The *square* outlined by *dashed lines* in the widefield plots (i, ii, iv, and v) represents the 6 × 6-mm region where the macular plots (vi and vii) were derived. The manually outlined ROI is shown using *white outlines* on the RNFL thickness and thickness probability plots. Note: Corresponding *scale bars* for the RNFL and RGC+ thickness maps and probability maps are shown on the *left*.

nal group and variability group, respectively, and eyes that satisfied both criteria were automatically assigned to the longitudinal group.

Methods Used for Detecting Progression

A customized program in MATLAB (MathWorks, Natick, MA) was used to manually coregister pairs of widefield and optic disc volume scans for the eyes in the longitudinal and variability groups using the retinal features (including blood vessels and the optic disc) visible on en face projection images (as in Fig. 1, left panels). For the widefield scans of eyes in the longitudinal group, another customized program in MATLAB was used to manually outline regions of observed or suspected glaucomatous damage after reviewing the information available from the second visit using a single summary image shown in Figure 2. The information in this summary image included the following (Roman numerals in parentheses indicate figure parts): (i) RNFL thickness plot; (ii) RNFL thickness probability plot; (iii) three vertical line B-scans taken through the center of the fovea and 1.5 mm on either side; (iv) en face projection image; (v) en face slab image of the inner retina (derived from the average intensity of a 52-µm slab below the inner limiting membrane[19]); (vi) macular retinal ganglion cell plus inner plexiform layer (RGC+) thickness plot; (vii) RGC+ thickness deviation probability plot; (viii) a circumpapillary circle B-scan; and (ix) cpRNFL thickness profile plot. On this summary image (Fig. 2), a grader was permitted to outline any region on the RNFL thickness, RNFL thickness probability plots, the en face projection, or slab images; the manually outlined ROI for this example is shown using white outlines. Note that although information about the macular RGC+ thickness from the summary image was reviewed, progressive change in the RGC+ thickness was not evaluated in this study. For

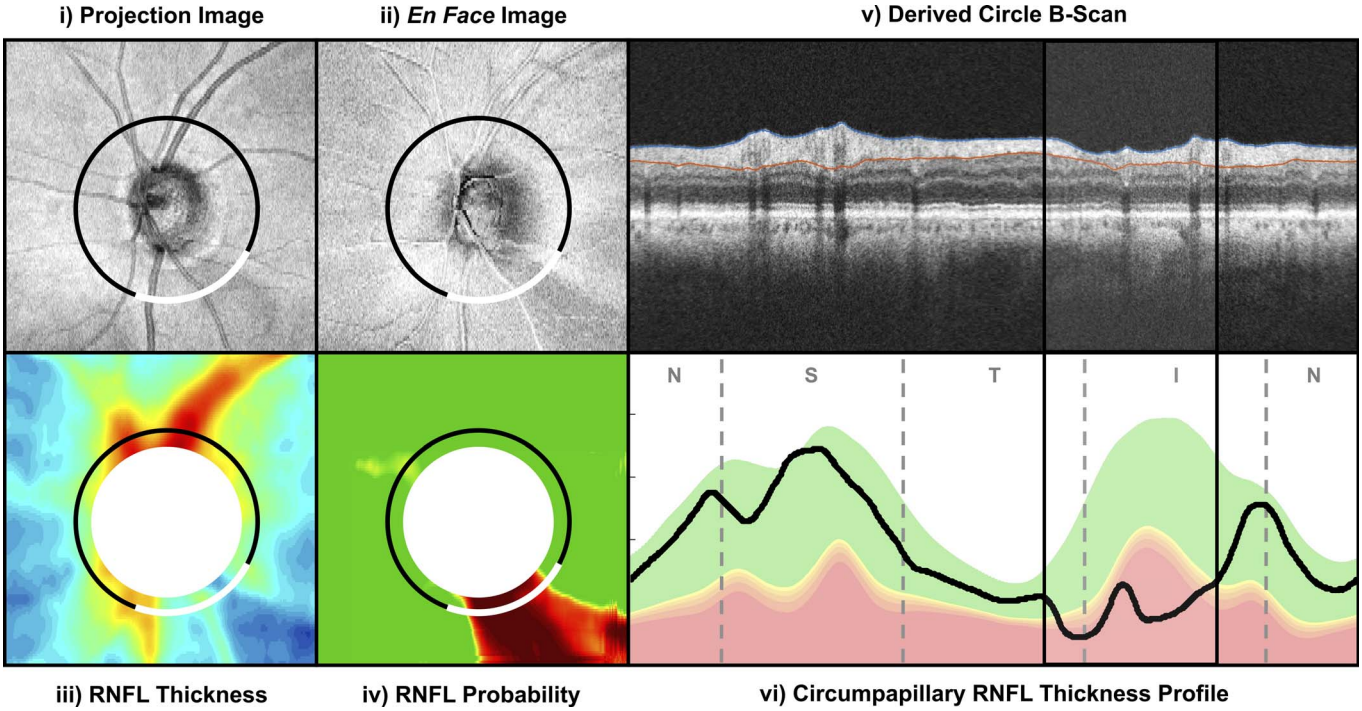

Figure 3. Information from the optic disc scan evaluated when manually identifying a ROI, including (i) en face projection image, (ii) en face slab image of the inner retina, (iii) RNFL thickness plot, (iv) RNFL probability plot, (v) derived circumpapillary circle B-scan, (vi) the corresponding circumpapillary RNFL thickness profile. The manually outlined ROIs are shown using *black rectangles* on the *right panels* (v, vi), and the corresponding region is shown using *white arcs* on the *left* and *middle panels* (i–iv).

the progression analysis, the RNFL thickness values (1) were averaged only within the overlapping regions between the two scans, so the same retinal locations were evaluated; (2) were averaged only within the central 10 × 7-mm region of each scan, which excluded the outer 1 mm from each edge to avoid edge artifacts; and (3) were excluded within a 3.4-mm radius of the optic disc center, as these values may be more variable. The averaged values were referred to as the $\text{wfRNFL}_{\text{ROI}}$ measurements.

For the optic disc scans, another customized MATLAB program was used to manually outline regions of observed or suspected glaucomatous damage for the eyes in the longitudinal group, after reviewing information available from the second visit using a different single summary image, shown in Figure 3. This summary image consisted of (i) en face projection image; (ii) en face slab image of the inner retina (derived from the average intensity of a 52-μm slab below the inner limiting membrane[19]); (iii) RNFL thickness plot; (iv) RNFL probability plot; (v) derived circumpapillary circle B-scan with a 3.4-mm radius averaged over an annulus 100-μm wide); (vi) the corresponding cpRNFL thickness profile. A grader was permitted to outline any region within the circumpapillary circle scan or RNFL thickness profile (an example of the manually outlined ROI is shown using black rectangles and white arcs in Fig. 3), and the averaged values of these regions were referred to as the $\text{cpRNFL}_{\text{ROI}}$ measurements. The circumpapillary RNFL thickness values averaged over the entire derived circle B-scan were referred to as the cpRNFL_{G} measurements. The manual delineation of the ROI(s) for both the widefield and optic disc scans were performed by experienced graders using only the information from the second visit.

Calculating Longitudinal SNRs

Longitudinal SNRs[20] for the $\text{wfRNFL}_{\text{ROI}}$, $\text{cpRNFL}_{\text{ROI}}$, and cpRNFL_{G} methods were derived to enable an equivalent comparison between them, since it accounts for between-method and between-individual differences in normal age-related changes and measurement variability. The longitudinal SNRs for each method (m) were calculated by first obtaining the difference in RNFL thickness between the two visits (δ), then dividing this difference by the follow-up interval (t) to obtain an estimate of its rate of

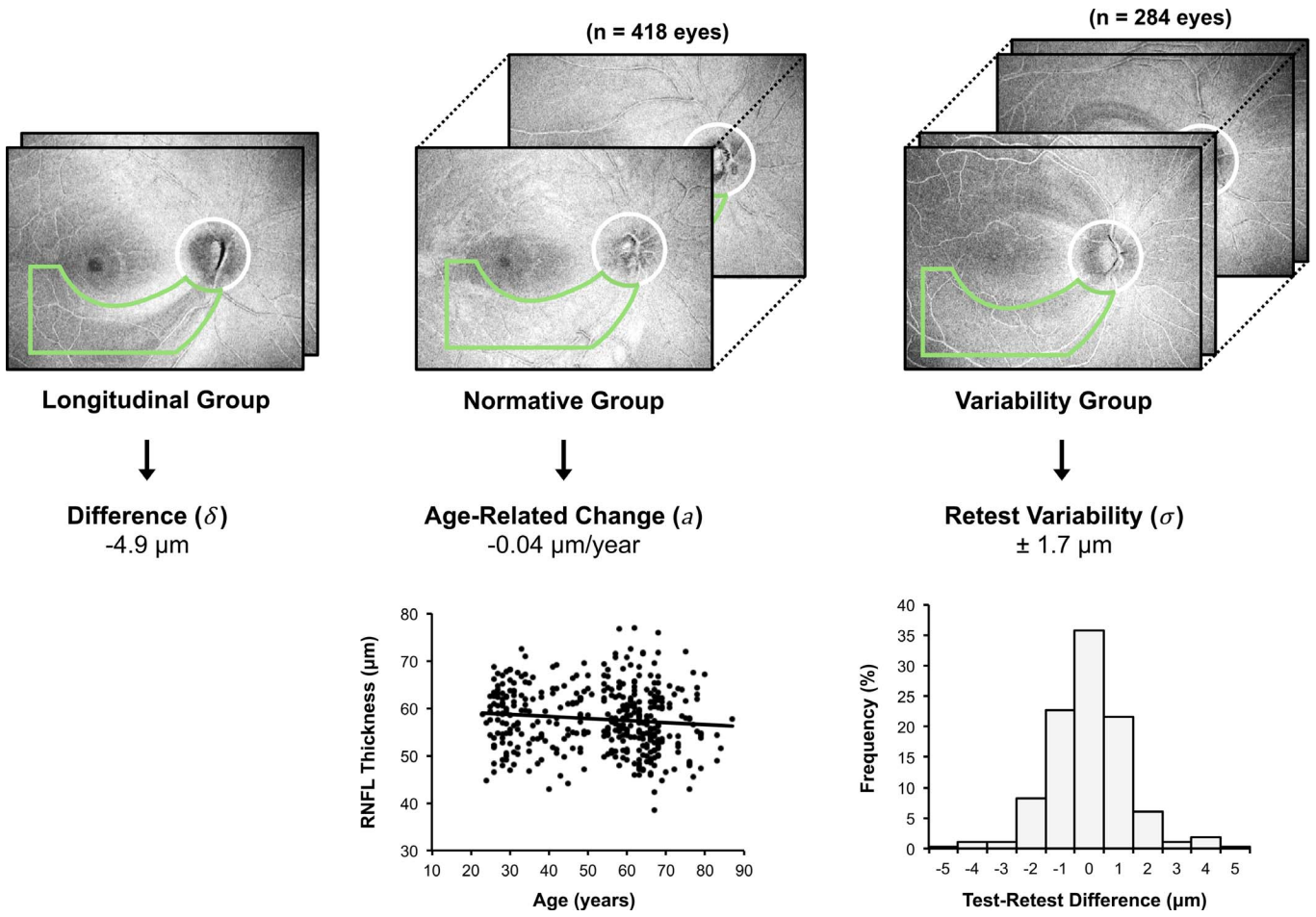

Figure 4. An example illustrating the process of obtaining parameters required to calculate longitudinal SNRs for a specific ROI (*green outline*) on widefield OCT scans of an eye in the longitudinal group (*left panel*). Age-related change estimates were obtained by obtaining the slope of a linear regression model fit between the average RNFL thickness of the ROI of each eye in the normative group against age (*middle panel*). Measurement variability estimates were derived from the standard deviation of the test-retest differences of the average RNFL thickness of the ROI for all eyes in the variability group.

change. This rate of change was then subtracted by an estimate of the normal rate of age-related change (a), before being divided by a corresponding estimate of measurement variability (σ). This can be expressed as:

$$\mathrm{SNR}_m = \frac{(\delta_m/t) - a_m}{\sigma_m}.$$

For the $\mathrm{wfRNFL_{ROI}}$ and $\mathrm{cpRNFL_{ROI}}$ methods, unique estimates of measurement variability and age-related change were determined for each eye in the longitudinal group based on the ROI manually outlined. These estimates were obtained using a process illustrated in Figure 4. Here, an inferior-temporal arcuate defect was manually outlined (a green outline; left panel) on a widefield scan. An individualized cross-sectional age-related change estimate of this ROI was obtained from the slope of a linear regression model fitted between the average RNFL thicknesses of this ROI from all the eyes in the normative group against age (illustrated in the middle panel of Fig. 4). A unique measurement variability estimate of the same ROI was obtained by calculating the standard deviation of the test-retest differences of the average RNFL thicknesses from all eyes in the variability group (illustrated in the right panel of Fig. 4; also described further in the Statistical Analysis section).

For the widefield scans, 284 eyes from 183 participants with a diagnosis of glaucoma or suspected glaucoma were included in the widefield scan variability group, which had OCT scans within a session. The median age of these participants was 62 years (interquartile range [IQR] = 48–69 years), and their median (IQR) visual field MD and pattern

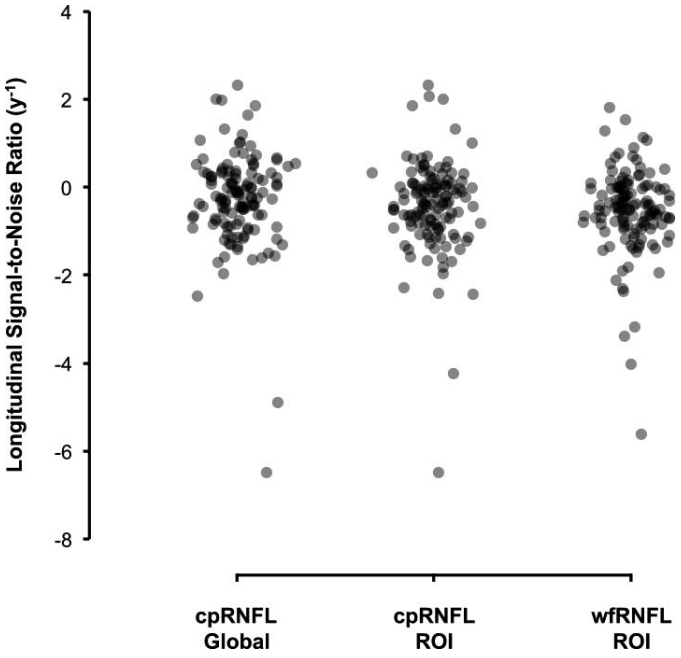

Figure 5. Distribution of the longitudinal SNRs of the change in the global cpRNFL thickness (*left*) and the ROI cpRNFL thickness derived from the optic disc scan (*middle*), and wfRNFL thickness using a ROI approach. More negative values indicate that a greater extent of change over time was detected relative to measurement variability and age-related changes.

standard deviation (PSD) were −2.43 dB (IQR = −5.84 to −0.87 dB) and 2.23 dB (IQR = 1.55–6.53 dB), respectively. A different, but overlapping, cohort of 321 eyes from 199 participants diagnosed with glaucoma or suspected glaucoma were included in the variability group for the optic disc scans. The median age of these participants was 62 years (IQR = 49–69 years), and their median visual field MD and PSD were −2.57 dB (IQR = −6.04 to −0.90 dB) and 2.27 dB (IQR = 1.55–6.54 dB), respectively. To obtain estimates of normal age-related changes for the widefield scans, 418 eyes from 418 participants were included, and their median age was 58 years (IQR = 38–66 years). For the optic disc scans, a different cohort of 394 eyes from 394 participants was included, and the median age of these participants was 47 years (IQR = 32–60 years).

Statistical Analysis

To account for the hierarchical nature of the test-retest standard deviation estimate (i.e., as two eyes from a single individual were sometimes included), a type of linear mixed model, a random intercept model, was used. Random intercept models were also used when comparing the longitudinal SNRs for the three methods in this study, nesting methods within eyes and within participants. All statistical analyses were performed using MATLAB and statistical analysis software (Stata; StataCorp LP, College Station, TX).

Results

Participant Characteristics

A total of 125 eyes of 82 participants with a clinical diagnosis of glaucoma or suspected glaucoma were included in the longitudinal group, which had both optic disc and widefield OCT scans at least 1 year apart. The median age of these participants was 61 years (IQR = 49–68 years), and they were seen over a median follow-up duration of 1.6 years (IQR = 1.1–2.0 years). The median visual field MD and PSD of these eyes were −2.22 dB (IQR = −4.69 to −0.49 dB) and 1.96 dB (IQR = 1.58–6.24 dB), respectively. The median baseline RNFL thickness for the $cpRNFL_G$, $cpRNFL_{ROI}$, and $wfRNFL_{ROI}$ methods were 85 μm (IQR = 66–97 μm), 82 μm (IQR = 56–97 μm), and 45 μm (IQR = 33–59 μm), respectively. The median rate of RNFL thickness change for these methods were −0.7 μm/year (−1.9 to 0.5 μm/year), −1.6 μm/year (−3.3 to 0.0 μm/year), and −0.6 μm/year (−1.1 to −0.1 μm/year), respectively.

Comparison of the Longitudinal SNR Ratio Between Methods

The distributions of the longitudinal SNR of each method are presented in Figure 5. The average longitudinal SNRs for the $cpRNFL_G$, $cpRNFL_{ROI}$, and $wfRNFL_{ROI}$ were −0.23 y^{-1}, −0.38 y^{-1}, and −0.57 y^{-1}, respectively, where more negative values indicate a greater extent of RNFL change detected relative to test-retest variability and age-related changes. The average longitudinal SNR of the $wfRNFL_{ROI}$ was significantly more negative than the $cpRNFL_{ROI}$ (−0.19 y^{-1}; 95% confidence interval [CI] = −0.33 to −0.05 y^{-1}; $P = 0.009$) and the $cpRNFL_G$ (−0.34 y^{-1}; 95% CI = −0.49 to −0.19 y^{-1}; $P < 0.001$). Note that the average longitudinal SNR was also significantly more negative for the $cpRNFL_{ROI}$ method than the $cpRNFL_G$ method (−0.15 y^{-1}; 95% CI = −0.24 to −0.07 y^{-1}; $P < 0.001$).

Examples of Findings in This Study

Two examples illustrating the superior ability of the $wfRNFL_{ROI}$ method for detecting progressive

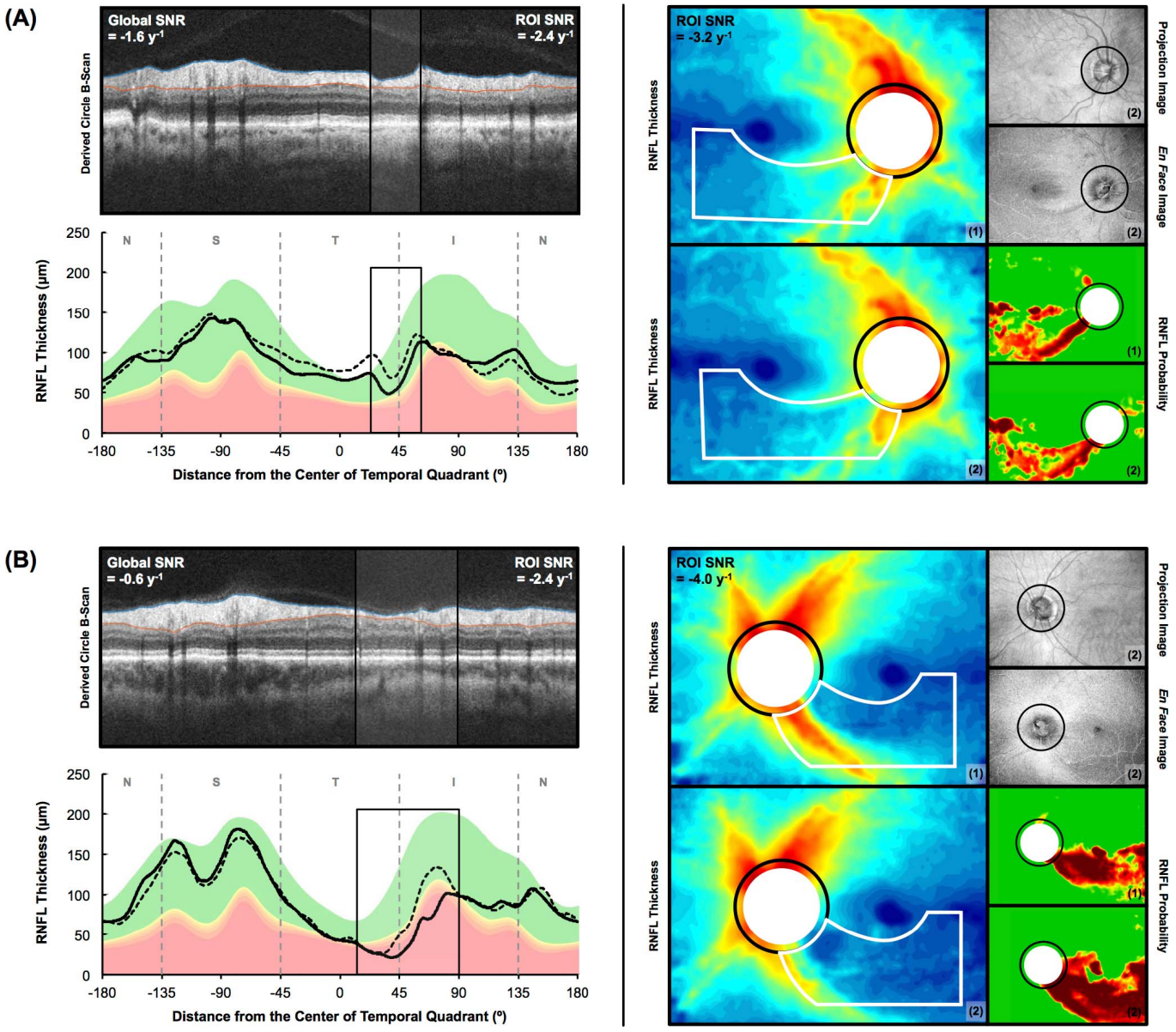

Figure 6. Two examples of glaucoma eyes where the ROI approach on the widefield scans (*right*) detected a greater extent of longitudinal RNFL thickness decline relative to age-related changes and measurement variability compared to the manual ROI approach and global thickness parameter on the circumpapillary circle scan derived from an optic disc scan (*left*), expressed using longitudinal SNR. In each example, the circumpapillary circle B-scan from the optic disc scan from the second visit and its corresponding RNFL thickness profile from the first and second visits (*dashed* and *solid black lines*, respectively) are shown on the *left panel*. The *right panel* shows wfRNFL thickness plots and thickness probability plots for the first and second visits (indicated by numbers in the parentheses), as well as the en face projection image and en face inner retina slab image.

changes compared to the $cpRNFL_{ROI}$ and $cpRNFL_{G}$ methods are shown in Figure 6, and the manually outlined ROIs for these defects are shown using white outlines on the widefield RNFL thickness plots and using black rectangles on the circumpapillary B-scan and RNFL thickness profiles. Both examples show eyes with an inferior-temporal arcuate RNFL defect, where a more negative longitudinal SNR was observed in both examples using the $wfRNFL_{ROI}$ method (−3.2 and −4.0 y^{-1}, respectively) compared to the $cpRNFL_{ROI}$ (−2.4 y^{-1} for both) and $cpRNFL_{G}$ methods (−1.6 and −0.6 y^{-1}, respectively).

Discussion

The findings of this study suggest that progressive RNFL thickness changes were better detected on widefield OCT scans than from a derived circle scan of optic disc scans using a manual ROI approach after accounting for measurement variability and age-related changes. This highlights the potential advantages of using widefield scans to monitor progressive glaucomatous damage, which may be gained by evaluating a larger proportion of the entire RGC axonal tract as compared to a single location with a circumpapillary circle scan.

To fully appreciate the implications of the findings of this study, it is important to understand the longitudinal SNRs that were evaluated. Longitudinal SNRs provide a normalized measure of the age-adjusted rate of change in RNFL thickness for an eye divided by the standard deviation of test-retest differences. This measure is distinguished from conventional SNRs or *z* scores, which can be used to represent a normalized measure of the *extent* of change relative to variability, rather than the *rate* of change. As such, longitudinal SNRs are not intended to provide an estimate of whether an individual eye has progressed or not but rather are simply used to compare the different methods evaluated in this study.

Recognizing this interpretation, we note that no prior progression study, to our knowledge, has compared the performance of RNFL thickness measurements from a three-dimensional 12 × 9-mm widefield volume scan against those from a two-dimensional circumpapillary circle scan. Studies that have compared RNFL thickness measurements from the entire three-dimensional 6 × 6-mm optic disc scan against the circumpapillary circle scans have also been scarce and inconclusive. One study suggested that local event-based analysis of the RNFL thickness maps on such optic disc scans detected the greatest number of glaucoma eyes as having progressed compared to event- and trend-based analysis of cpRNFL thickness measurements,[9] whereas the results from another study suggested that trend-based analysis of the global cpRNFL thickness performed best.[12] However, neither study reported the statistical significance of these differences nor the specificities of these methods (required for equivalent comparisons), making it difficult to determine whether the analysis of the entire RNFL thickness map or cpRNFL thickness values is better based on those studies.

The improved ability for the progressive RNFL thickness changes to be detected on the widefield scans may be attributed to the greater reduction in measurement variability through averaging measurements over a substantially larger scanned area. The number of A-scans within the entire widefield scan (after excluding 1 mm from each edge) is nearly 20-fold that within the derived circle scan from the optic disc scan (averaged over a 100-μm annulus). It may also be attributed to the fact that progressive RNFL thickness change is more accurately captured when evaluated along a much larger portion of its entire axonal tract using the widefield scans, enhanced by the use of a manual ROI approach where a greater extent of information was available.[17,18] However, it remains to be determined how measurements from a single high-resolution, frame-averaged circle scan (e.g., those obtained using the Spectralis HRA+OCT device; Heidelberg Engineering GmbH, Heidelberg, Germany) performs against a widefield scan approach, and future studies are required to evaluate this.

The findings of this study underscore the potential advantage of using widefield scans for the challenging task of detecting progressive glaucomatous RNFL changes. The advantages of widefield scans have also been seen in recent studies that showed its improved ability to detect glaucomatous damage at cross-section.[14–16] This study also highlights the advantages of a ROI approach over the conventional use of the global cpRNFL thickness parameter,[17,18] gained by making full use of the OCT information available along with knowledge about the patterns of glaucomatous damage. However, it should be acknowledged that the comparisons between the average longitudinal SNRs of the methods performed in this study are meant to provide an evaluation of the potential value of each approach at the population-average level. The use of a dichotomized outcome measure of whether progression has occurred or not would have substantially diluted the statistical power to appreciate the true value of each method,[21] especially given that the majority of glaucoma eyes under routine clinical care often progress slowly.[22] Nonetheless, future studies are required to better understand the implications of these findings at the individual level, potentially through using trend- or event-based analyses of ROIs of longitudinal data (including a greater number of visits and follow-up duration) when compared to current methods. In addition, future studies are also required to determine the generalizability (performing intra- and intergrader

assessments) of the manual ROI approach used in this study.

Several limitations of this study should be acknowledged when interpreting its findings. First, the age-related changes estimates were obtained in two different cohorts of healthy eyes. However, the sample size of both cohorts was relatively large ($n \geq 394$), and therefore substantial differences in estimates of age-related changes are unlikely. Although longitudinal estimates of age-related change would have been more ideal compared to the cross-sectional estimates used in this study, it is unlikely that its use would significantly change the conclusions of this study since the same eyes were used to obtain the estimates for all three methods. Second, measurement variability estimates were also obtained in two different, but overlapping cohorts of glaucoma eyes. However, a total of 258 eyes were included for estimating the measurement variability of both the widefield and optic disc scans (representing 90% and 80% of the entire cohort, respectively), thus providing variability estimates from two very similar cohorts. It would also have been ideal if these estimates were obtained from a short-term test-retest cohort (rather than the intrasession estimates in this study), but this would also be unlikely to have changed the conclusions in this study given how the variability estimates were obtained from a very similar cohort of eyes. Third, progressive changes in the longitudinal group were only evaluated between two visits and over a relatively short duration, although increasing the number of visits and duration of follow-up would likely improve the precision of the change estimates without also altering the conclusions of this study. Finally, within-session estimates of measurement variability were used instead of short-term between-session estimates, which would be more representative of the extent of variability observed in a longitudinal cohort. Nevertheless, the within-session variability estimates were used when calculating the longitudinal SNRs for both the RNFL thickness changes from the widefield and optic disc scans (as a common denominator) and is thus unlikely to significantly affect the conclusions reached in this study.

In conclusion, the findings of this study using a manual ROI approach suggest that progressive RNFL changes in glaucoma eyes can be better detected using widefield OCT scans than derived circumpapillary circle scans from optic disc scans. These findings highlight potential advantages of using widefield scans for the challenging task of detecting disease progression in the clinical management of glaucoma.

Acknowledgments

Supported by a National Institutes of Health Grant R01-EY-02115 (DCH), Lary Stromfeld Research Fund of NYEEI (RR), and a National Health and Medical Research Council Early Career Fellowship 1104985 (ZW).

Disclosure: **Z. Wu**, None; **D.S.D. Weng**, None; **A. Thenappan**, None; **R. Rajshekhar**, None; **R. Ritch**, None; **D.C. Hood**, Topcon, Inc. (F, C, R), Heidelberg Engineering (F, C, R)

References

1. Hood DC. Improving our understanding, and detection, of glaucomatous damage: an approach based upon optical coherence tomography (OCT). *Prog Retin Eye Res*. 2017;57:46–75.
2. Kotowski J, Wollstein G, Ishikawa H, Schuman JS. Imaging of the optic nerve and retinal nerve fiber layer: an essential part of glaucoma diagnosis and monitoring. *Surv Ophthalmol*. 2014;59:458–467.
3. Grewal DS, Tanna AP. Diagnosis of glaucoma and detection of glaucoma progression using spectral domain optical coherence tomography. *Curr Opin Ophthalmol*. 2013;24:150–161.
4. Vianna JR, Chauhan BC. How to detect progression in glaucoma. *Prog Brain Res*. 2015;221:135–158.
5. Medeiros FA. Biomarkers and surrogate endpoints in glaucoma clinical trials [published online ahead of print July 7, 2014]. *Br J Ophthalmol*. https://doi.org/101136/2014:bjophthalmol-2014-305550.
6. Medeiros FA. Biomarkers and surrogate endpoints: lessons learned from glaucoma. *Invest Ophthalmol Vis Sci*. 2017;58:BIO20–BIO26.
7. Meira-Freitas D, Lisboa R, Tatham A, et al. Predicting progression in glaucoma suspects with longitudinal estimates of retinal ganglion cell counts. *Invest Ophthalmol Vis Sci*. 2013;54:4174–4183.
8. Miki A, Medeiros FA, Weinreb RN, et al. Rates of retinal nerve fiber layer thinning in glaucoma

suspect eyes. *Ophthalmology*. 2014;121:1350–1358.
9. Na JH, Sung KR, Baek S, et al. Progression of retinal nerve fiber layer thinning in glaucoma assessed by cirrus optical coherence tomography-guided progression analysis. *Curr Eye Res*. 2013; 38:386–395.
10. Yu M, Lin C, Weinreb RN, et al. Risk of visual field progression in glaucoma patients with progressive retinal nerve fiber layer thinning: a 5-year prospective study. *Ophthalmology*. 2016; 123:1201–1210.
11. Lin C, Mak H, Yu M, Leung CK-S. Trend-based progression analysis for examination of the topography of rates of retinal nerve fiber layer thinning in glaucoma. *JAMA Ophthalmol*. 2017; 135:189–195.
12. Shin JW, Sung KR, Lee J, Kwon J. Factors associated with visual field progression in cirrus optical coherence tomography-guided progression analysis: a topographic approach. *J Glaucoma*. 2017;26:555–560.
13. Yang Z, Tatham AJ, Zangwill LM, et al. Diagnostic ability of retinal nerve fiber layer imaging by swept source optical coherence tomography in glaucoma. *Am J Ophthalmol*. 2015;159:193–201.
14. Hood DC, De Cuir N, Blumberg DM, et al. A single wide-field oct protocol can provide compelling information for the diagnosis of early glaucoma. *Trans Vis Sci Tech*. 2016;5:4.
15. Muhammad H, Fuchs TJ, De Cuir N, et al. Hybrid deep learning and a single wide-field OCT scan accurately classifies glaucoma suspects. *J Glaucoma*. 2017;26:1086–1097.
16. Lee WJ, Na KI, Kim YK, et al. Diagnostic ability of wide-field retinal nerve fiber layer maps using swept-source optical coherence tomography for detection of preperimetric and early perimetric glaucoma. *J Glaucoma*. 2017;26:577–585.
17. Hood DC, Xin D, Wang D, et al. A region-of-interest approach for detecting progression of glaucomatous damage with optical coherence tomography. *JAMA Ophthalmol*.133: 2015:1–7.
18. Thenappan A, De Moraes CG, Wang DL, et al. Optical coherence tomography and glaucoma progression: a comparison of a region of interest approach to average retinal nerve fiber layer thickness. *J Glaucoma*. 2017;26:473–477.
19. Hood DC, Fortune B, Mavrommatis MA, et al. Details of glaucomatous damage are better seen on OCT en face images than on OCT retinal nerve fiber layer thickness maps. *Invest Ophthalmol Vis Sci*. 2015;56:6208–6216.
20. Gardiner SK, Fortune B, Demirel S. Signal-to-noise ratios for structural and functional tests in glaucoma. *Trans Vis Sci Tech*. 2013;2:3.
21. Royston P, Altman DG, Sauerbrei W. Dichotomizing continuous predictors in multiple regression: a bad idea. *Stat Med*. 2006;25:127–141.
22. Chauhan BC, Malik R, Shuba LM, et al. Rates of glaucomatous visual field change in a large clinical population. *Invest Ophthalmol Vis Sci*. 2014;55:4135–4143.